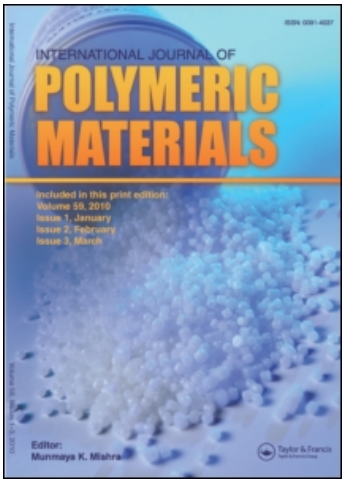

International Journal of Polymeric Materials
Publication details, including instructions for authors and subscription information:
http://www.informaworld.com/smpp/title~content=t713647664

Effect of Compatibilizer Type on Properties of 70:30 Polyamide 6/Polypropylene/MMT Nanocomposites

Norhayani Othman[a]; Azman Hassan[a]; Abdul Razak Rahmat[a]; Mat Uzir Wahit[a]
[a] Faculty of Chemical and Natural Resources Engineering, Universiti Teknologi Malaysia,

To cite this Article Othman, Norhayani , Hassan, Azman , Rahmat, Abdul Razak and Wahit, Mat Uzir(2007) 'Effect of Compatibilizer Type on Properties of 70:30 Polyamide 6/Polypropylene/MMT Nanocomposites', International Journal of Polymeric Materials, 56: 9, 893 — 909
To link to this Article: DOI: 10.1080/00914030601123377
URL: http://dx.doi.org/10.1080/00914030601123377

International Journal of Polymeric Materials, 56:893–909, 2007

ISSN: 0091-4037 print/1563-535X online
DOI: 10.1080/00914030601123377

Taylor & Francis
Taylor & Francis Group

Effect of Compatibilizer Type on Properties of 70:30 Polyamide 6/Polypropylene/MMT Nanocomposites

Norhayani Othman
Azman Hassan
Abdul Razak Rahmat
Mat Uzir Wahit
Faculty of Chemical and Natural Resources Engineering,
Universiti Teknologi Malaysia

PA6/PP nanocomposites with either polyethylene octene elastomer grafted maleic anhydride (POEgMAH) or PP grafted maleic anhydride (PPgMAH) as compatibilizer were prepared using co-rotating twin-screw extruder followed by injection molding. The mechanical and microstructural properties of the composites were investigated by means of tensile, flexural, and impact testing and by scanning electron microscopy (SEM). X-ray diffraction (XRD) was used to characterize the formation of nanocomposites. The result indicated that the miscibility of PA6/PP nanocomposites was improved with the addition of POEgMAH and PPgMAH. The impact strength of PA6/PP nanocomposite with POEgMAH increased about 5 times higher than uncompatibilized composite. Increment in tensile properties was observed when PPgMAH was used as compatibilizer. XRD results revealed that PA6/PP nanocomposites were successfully formed. Uniform dispersion of PP in matrix were observed through SEM, which showed the improvement of the compatibility between polymers.

Keywords: compatibilizers, nanocomposites, polyamide-6, polypropylene

INTRODUCTION

Polymer nanocomposites, particularly polymer clay nanocomposites that consist of layered silicates, have received considerable attention due to their dramatic improvement in material properties by addition of just a small fraction of clay to a polymer matrix. Although extensive

Received 24 October 2006; in final form 1 November 2006.
Address correspondence to Azman Hassan, Faculty of Chemical and Natural Resources Engineering, Universiti Teknologi Malaysia, 81310 Skudai, Johor Bahru, Malaysia. E-mail: azmanh@fkkksa.utmmy

studies on single polymer matrix nanocomposites have been reported [1–3], not many studies on nanocomposites based on polymer blends have been carried out.

Polyamide (PA) blended with polypropylene (PP) leads to improved chemical and moisture resistance, dimension stability, and reduced cost of the corresponding neat polymer [4–12]. However, PA and PP are not miscible. Therefore, addition of a third component known as compatibilizer is generally required to achieve those advantages. Successful approaches involve addition of polypropylene grafted with maleic anhydride (PPgMAH) as a compatibilizer to the blends [5–9]. Nevertheless, high levels of toughness can only be achieved by addition of an appropriate rubber that can function as an impact modifier. Maleated rubbers such as ethylene propylene random copolymers (EPRgMAH), and maleated polyethylene octene elastomer (POEgMAH) are known to act both as an impact modifier and compatibilizer for PA6/PP blends [9–13].

These functionalized polymers copolymerize "in situ" by grafting with PA6, giving rise to an interfacial adhesion between the polymers, and leading to a finer dispersion of the dispersed particles in the matrix, which are believed to be essential for promoting toughness. Furthermore, presence of compatibilizer also would alter the clay dispersion and improve compatibility between dispersed layered silicates and polymers, which result in significant changes in properties [7,10,13–14]. Therefore, mutual miscibility and adhesion of the constituents are the crucial factors influencing the structure and final properties of the composites.

In a recent publication, we reported on the mechanical and morphological behavior of toughened PA6/PP nanocomposites. Three compositions were studied: 80, 70, and 60 wt% PA. It was revealed that 70:30 PA6/PP showed the highest impact strength for both toughened blends and nanocomposites [14]. Therefore the work described in this article focuses on comparing the effects of two types of compatibilizers, PPgMAH and POEgMAH, on the mechanical, thermal, and morphology of 70:30 PA6/PP nanocomposites.

EXPERIMENTAL

Materials

The blends used in this work are described in Table 1. The PA6 (Amilan CM 1017) is a commercial product from Toray Nylon Resin AMILAN, Japan. The MFI of PA6 is 35 g/10 min at 230°C and 2.16 kg load and the density is 1.14 g/cm^3. The PP (SM 240) was

TABLE 1 Blends Used in this Work (wt%)

Formulation	PA6	PP	PPgMAH	Organoclay	POEgMAH
PA6/PP/FA4	67.2	28.8	—	4	—
PA6/PP/FA4/C5	63.7	27.3	5	4	—
PA6/PP/FA4/E10	60.2	25.8	—	4	10

obtained from Titan PP Polymers, Johor, Malaysia. The melt flow index (MFI) and density of PP is 25 g/10 min (at 230°C and 2.16 kg load) and 0.9 g/cm^3, respectively. PP grafted with maleic anhydride (PPgMAH) used was Orevac CA 100 with $\sim$1 wt% of maleic anhydride (MAH) produced by ATOFINA, France. The polyethylene octene random (11 wt% octene) copolymer grafted with maleic anhydride (POEgMAH) was made by DuPont (Fusabond MN493D) with density 0.87 g/cm^3. The organoclay (Nanomer 1.30 TC) used was a commercial product from Nanocor Inc. USA. This organoclay is a white powder containing montmorillonite (MMT) (70 wt%) intercalated by octadecylamine (30 wt%).

Specimen Preparation

PA6, PP, organoclay, PPgMAH, or POEgMAH were dry blended in a tumbler mixer according to the compositions in Table 1. The polymers and additives were then melt blended by simultaneous addition of all components into a Berstoff co-rotating twin screw extruder. The barrel temperatures were gradually increased from hopper to die at 200, 220, 230, and 240°C and the rotating screw was 50 rpm. Prior to extrusion, PA6 pellets were dehumidified by using a dryer at 80°C for 8 h. The pelletized materials were dried and injection molded into a standard tensile, flexural, and impact specimen using a JSW Model N100B II injection molding machine with the barrel temperature of 210–240°C.

Materials Characterization

Mechanical Testing

Tensile and flexural tests were carried out according to ASTM D638 and ASTM D790 method respectively, using an Instron 5567 Universal Testing Machine under ambient conditions. The crosshead speed for the tensile test was 50 mm/min, and for the flexural test it was set at 3 mm/min. The Izod impact test was carried out on notched specimens using Toyoseiki impact tester at ambient conditions

according to ASTM D256. The values reported in this study are the average of five specimens tested.

Molau Test

The Molau test was conducted by mixing about 0.8 g pellets of uncompatibilized PA6/PP nanocomposites with 20 mL of formic acid. The mixture was placed in a test tube at room temperature and left for 2 weeks. The same procedure was repeated for compatibilized PA6/PP nanocomposites.

Infrared Spectroscopy (FTIR)

FTIR spectra of the polymer blends and undiluted component from Molau test were carried out on a Perkin Elmer spectrometer, performing 10 scans, resolution 4 cm^{-1}, using sample film prepared on KBr plates.

X-Ray Diffraction (XRD)

X-ray diffraction was performed with a Siemens XRD. The XRD diffraction patterns were recorded with a step size of 0.02° from $2\theta = 2$ to 10°. The interlayer spacing of organoclay was derived from the peak position (d_{001}-reflection) in XRD diffractograms according to the Bragg equation.

Microscopy Examination (SEM)

The morphology of the blends was examined using a Philips scanning electron microscope. Samples were cryogenically fractured in liquid nitrogen and etched in hot decalin for 3 h to extract the PP phase. Samples were coated with gold prior to examination under the electron beam. An operating voltage of 30 kV and a magnification of 1000× were used.

Differential Scanning Calorimeter (DSC)

Analysis of the melting and crystallization behavior of the blends and nanocomposites was carried out using a Perkin-Elmer DSC7 with temperature calibration by indium. All experiments were carried out under a nitrogen atmosphere. All specimens were in the range of 6–10 mg in weight. Samples were heated at a heating rate of 10°C/min from 30°C to 250°C and held for 1 min. The samples were then cooled to 30°C and heated for a second time to 250°C at a heating rate of 10°C/min in order to erase the thermal history. The melting temperatures (T_m) and crystallization temperatures (T_c) were taken as the temperature corresponding to the peak values of melting endotherms and exotherms, respectively. The degree of crystallinity X_c was

calculated as the ratio of the melting enthalpies subdivided by weight fraction w_i of the respective component in the blend, $X_c = \Delta H/(w_i \Delta H_o)$, where ΔH_o is the melting enthalpy of 100% crystalline polymer. 209 J/g and 190 J/g are the melting enthalpies of completely crystalline PP and PA6, respectively [7].

RESULT AND DISCUSSION

Mechanical Properties

The mechanical properties of uncompatibilized and compatibilized PA6/PP nanocomposites are shown in Figures 1–3. It can be seen from Figure 1 that the tensile strength and Young's modulus increased with incorporation of PPgMAH into the PA6/PP nanocomposites. The possible explanation for the increment in tensile strength is the improvement in interfacial adhesion between PA6 and PP, as well as greater interaction between PA6/PP blend and organoclay. The maleic anhydride groups of PPgMAH are able to react with PA6 amine terminal group to form PA6gPP copolymer. Besides that, some of the maleic anhydride groups of PPgMAH may also react with the octadecylamine group of the interacalated organoclay (Figure 4). Such interaction leads the organoclay particles to randomize exfoliated among the matrix, resulting in more efficient reinforcement effect. On the other hand, the tensile strength and Young's modulus decreased with incorporation of POEgMAH into PA6/PP nanocomposites. Although POEgMAH

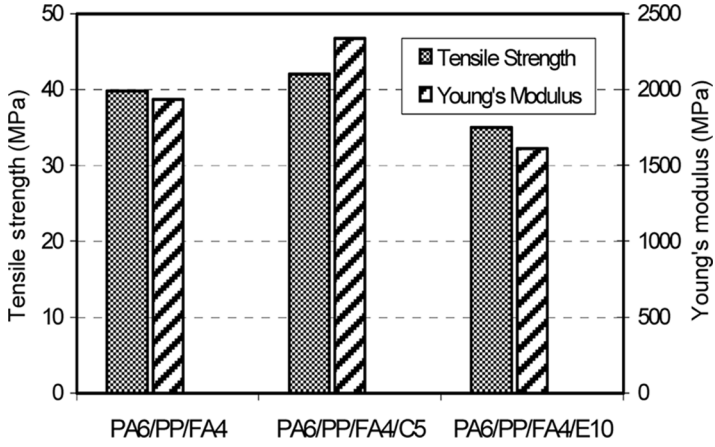

FIGURE 1 The effect of compatibilizer on tensile strength and Young's modulus.

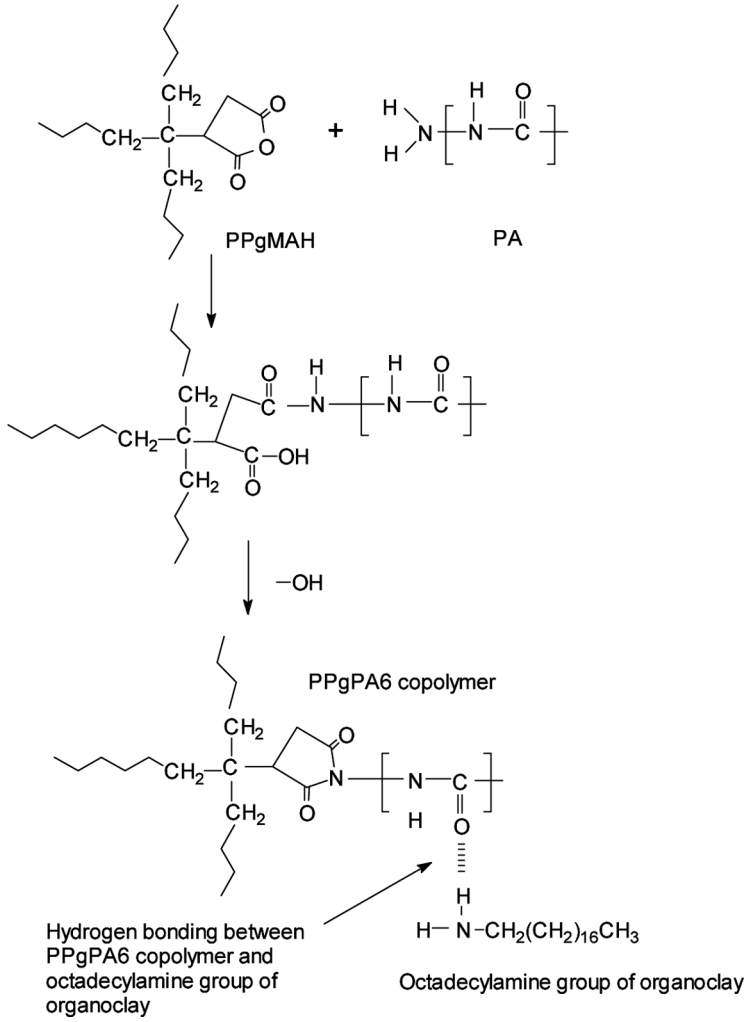

FIGURE 2 The effect of compatibilizer on flexural strength and flexural modulus.

improved the interaction between PA6 and PP, being a thermoplastic elastomer, it was not surprising that the modulus and strength of POEgMAH are lower than those of both PA6 and PP. The study by Zeng et al. [9] showed that the Young's modulus of PP/PA6 blend decreased upon the addition of POEgMAH. Li et al. [15] reported that when modified POE was used in $BaSO_4$ filled ternary composite, the

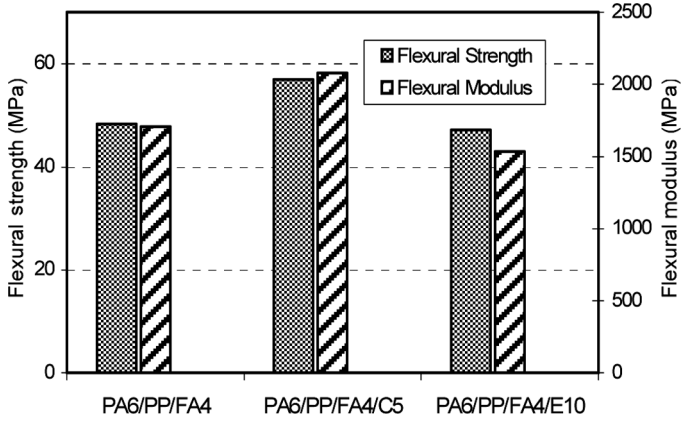

FIGURE 3 The effect of compatibilizer on impact strength and elongation at break.

fillers became encapsulated by the modified POE promoting a core-shell structure. This morphology was believed to be another reason responsible for reducing the modulus of the composite. The soft layer of elastomer adhered to the surfaces of the filler and inhibited the stiffening action of the filler particles resulting in lower modulus.

The effects of PPgMAH and POEgMAH compatibilizer on flexural strength and modulus of PA6/PP nanocomposites are shown in Figure 2. Flexural strength and modulus increased with the addition

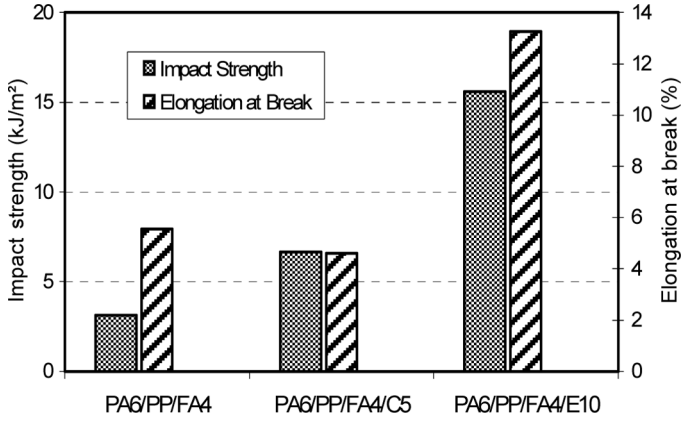

FIGURE 4 Formation of PA6gPOE copolymer and interaction with octadecylamine group from organoclay.

of PPgMAH. However, the flexural properties decreased when compatibilized by POEgMAH. These trends are similar to that of the tensile strength and Young's modulus.

The incorporation of POEgMAH or PPgMAH increased the impact strength of PA6/PP nanocomposites respectively (Figure 3). The impact strength of PPgMAH compatibilized nanocomposites increased by nearly 110% as compared to uncompatibilized nanocomposites. The improvement in impact strength of compatibilized nanocomposites is attributed to the improved adhesion between PA6 and PP as good adhesion is needed for effective stress transfer in immiscible blends [16].

However, a higher improvement of about 400% was obtained using POEgMAH, which is a functionalized elastomer. Zeng et al. [9] reported a similar trend whereby the POEgMAH compatibilized PP/PA6 blend was nearly 4 times higher than PPgMAH compatibilized PP/PA6 blend. They reported that POEgMAH encapsulated the dispersed PA6, which implies the existence of an interphase between PP and PA6. Besides being located at the interface between PA and PP, the compatibilizer also could be located at the surface or interlayer of layered silicates due to interaction of maleic anhydride group with the octadecylamine groups from the organoclay forming core-shell inclusion structure. The POEgMAH rubber that encapsulated around organoclay particles would increase the deformation ability of the matrix around filler particles as a result of the soft layer of elastomer adhering to the surfaces of filler, thus higher impact strength is found in core shell morphology. According to Li et al. [15] the encapsulation structure results in higher impact strength as a result of increased apparent volume fraction of elastomer, which decreased the distance between elastomer particles.

Figure 3 also shows that the elongation at break of the nanocomposites decreased with incorporation of PPgMAH, but increased when POEgMAH used. The results suggest that the addition of PPgMAH were not effective in improving the ductility of nanocomposites at low strain rate.

Molau Test

Molau test is used to verify the presence of graft copolymer in polymer system [17]. In the present study, the test was conducted to confirm the formation of graft copolymer between PA6 and POEgMAH or PPgMAH. The uncompatibilized nanocomposites were placed in formic acid, as formic acid is a solvent for PA6 and nonsolvent for PP and rubber. Within 1–3 h a phase separation was observed in the uncompatibilized PA/PP nanocomposites, the PA6 dissolved in formic acid

whereas other insoluble constituents were separated and floated on the top. This proves the incompatibility between PA6 and PP because phase separation occurred easily within 1–3 h. When the same procedure was repeated for the compatibilized nanocomposites, a stable emulsion in formic acid was obtained. This indicates that graft copolymer exist in compatibilized composites after the melt blending.

Infrared Spectroscopy Characterization

In order to confirm the existence of graft copolymer in compatibilized nanocomposites, FTIR test were conducted. Figure 5 shows the FTIR spectra of the insoluble fraction extracted from formic acid solution of the uncompatibilized and compatibilized nanocomposites from Molau test.

The IR characteristic bands are $\sim 1640\,cm^{-1}$ and $1540\,cm^{-1}$ corresponding to C=O and N–H of PA6 [17], C–H at $2930\,cm^{-1}$ and a broad peak at $3450\,cm^{-1}$, as well as weak peak at $1640\,cm^{-1}$ most probably corresponding to O–H and C=O from formic acid. As can be seen from spectrum (a), the absence of peak at $1540\,cm^{-1}$ which is an amide II

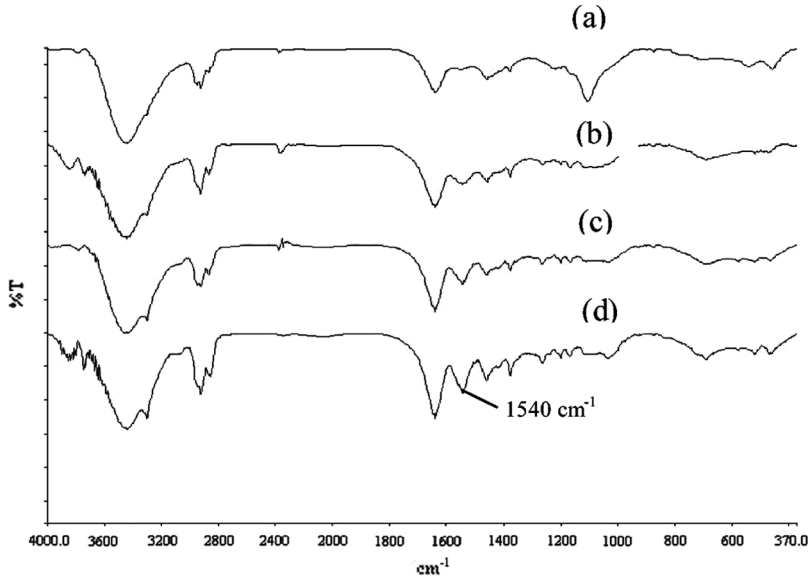

FIGURE 5 FTIR spectra of (a) uncompatibilized PA6/PP, (b) uncompatibilized PA6/PP nanocomposite, (c) PPgMAH compatibilized PA6/PP nanocomposite, and (d) POEgMAH compatibilized PA6/PP nanocomposite.

band, indicates that the PA6 in the PA6/PP blend was completely dissolved in formic acid. However, for uncompatibilized PA6/PP nanocomposites ((b)), a weak peak at 1540 cm^{-1} appeared. This may be simply due to the fact that the PA6 was not removed completely by formic acid. On the other hand, from the spectrum of the compatibilized blends (spectra (c) and (d)), the presence of the strong peak at 1640 cm^{-1} and 1540 cm^{-1} are due to the amide I and II bands of PA6. This indicates that the terminal amino groups in PA6 were probably involved in the formation of the imide linkage [5,17–19].

X-Ray Diffraction

Figure 6 shows the XRD patterns in the range of $2\theta = 2$–10° for uncompatibilized and compatibilized PA6/PP nanocomposites. The XRD spectrum of the organoclay exhibited a broad intense peak at around $2\theta = 3.52$ corresponding to a basal spacing of 2.48 nm. The XRD spectra of uncompatibilized and compatibilized PA6/PP nanocomposite did not show any obvious peak. It indicates that the organoclay structure has exfoliated. Wu et al. [2] and Cho and Paul [3] reported similar observations in the cases of PA1012 nanocomposites and PA6 nanocomposite, respectively. The absence of the characteristic clay d_{001} peak indicates that organoclay structure has exfoliated and dispersed randomly in PA1012 and PA6, respectively. Note that this XRD observation does not deliver any information about the change in organoclay dispersion with presence of different compatibilizer. However, Chow et al. [7,10] reported through their

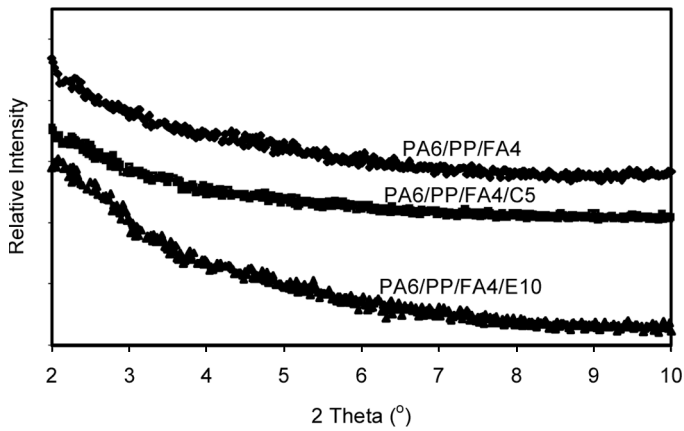

FIGURE 6 XRD pattern for uncompatibilized and compatibilized PA6/PP nanocomposites.

TEM observation that the incorporation of compatibilizer, either PPgMAH or EPRgMAH, leads to a more pronounced exfoliation of the organoclay as compared to uncompatibilized PA6/PP nanocomposite where partly intercalated/exfoliated structure was observed. In order to confirm the exfoliated structure, the dispersibility of silicate layers should also be observed by TEM. It is a better tool to monitor dispersion because the clay platelets can be seen. However, in our study TEM was not done.

Phase Morphology

The SEM micrographs of un-etched and etched fracture surfaces of uncompatibilized and compatibilized PA6/PP nanocomposites are shown in Figures 7 (a) to (c) and Figures 8 (a) to (d). Figure 7 (a) to (c) show the un-etched fracture surface of uncompatibilized and compatibilized PA6/PP nanocomposites. From uncompatibilized PA6/PP

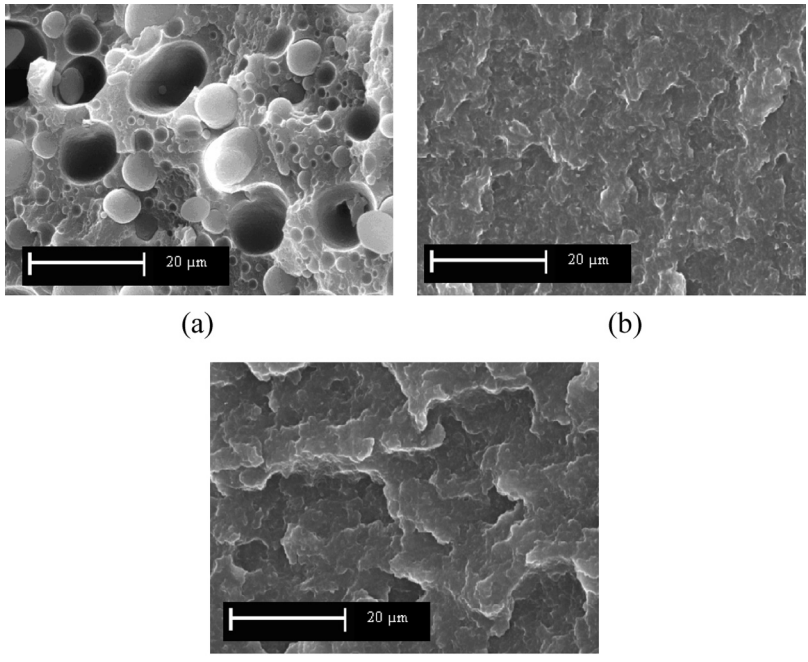

FIGURE 7 SEM micrographs of cryo-fractured surfaces of uncompatibilized and compatibilized nanocomposites (a) PA6/PP/organoclay, (b) PA6/PP PPgMAH/organoclay, (c) PA6/PP POEgMAH/organoclay.

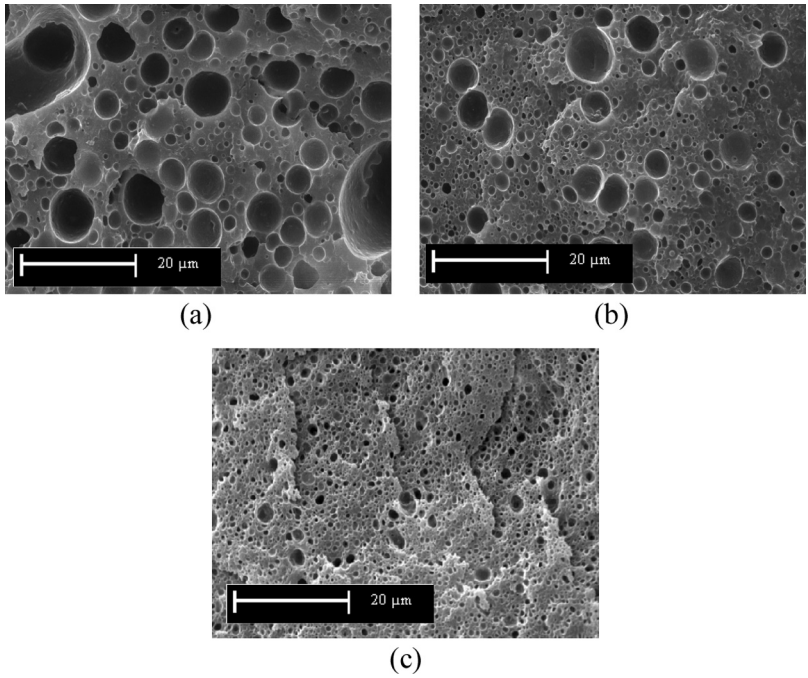

FIGURE 8 SEM micrographs of cryo-fractured surfaces of uncompatibilized and compatibilized nanocomposites extracted by decalin (a) PA6/PP/organoclay, (b) PA6/PP/PPgMAH/organoclay, (c) PA6/PP/POEgMAH/organoclay, (d) PA6/PP/PPgMAH/POEgMAH/organoclay.

nanocomposites micrograph it can be seen that poor adhesion between large spherical PP particles and matrix, which is clearly noted from the smooth fracture surface where PP particles were pulled from matrix. The easy detachment of PP from the PA6 matrix, Figure 7 (a), indicates a very weak interfacial adhesion. Uncompatibilized PA6/PP blends usually show a coarse dispersion of the minor phase in the matrix owing to the inherent incompatibility [7]. Figure 7 (b) and (c) show a more homogeneous fracture surfaces of compatibilized PA6/PP nanocomposites, which indicates the presence of interaction and better adhesion between PA6 and PP phase.

The compatibilizing effect can clearly be observed after etching. The etched surfaces showed dark circular holes, which represent the PP particles as the decalin dissolved the PP phase alone but did not dissolve the PA6 or rubber. From Figures 8 (b) and (c) it can be seen that the incorporation of compatibilizer, either PPgMAH or POEgMAH, leads to a decrease in PP particles size. This indicates that

TABLE 2 Particles Sizes of PP in Uncompatibilized and Compatibilized PA6/PP Nanocomposites

Blend	Particles counts	Diameter range (μm)	Average particle diameter	PP (μm)
PA6/PP/FA4	140	1.08–15.07	4.09	
PA6/PP/FA4/C5	249	0.71–13.38	2.34	
PA6/PP/FA4/E10	800	0.56–5.54	1.20	

PPgMAH and POEgMAH have a pronounced effect on better interfacial adhesion between PP and PA6. This observation is in agreement with the studies obtained by other researches on compatibilizing effect [6–8, 10,11]. The added compatibilizer plays major role in lowering interfacial tension and thereby forming finer morphology [8]. The SEM mircographs demonstrate that the addition of compatibilizer suppressed the coalescence and is in accordance with the results from Molau test and IR spectroscopy, thus suggesting the formation of an interfacial copolymer.

As shown in Table 2, in blends where POEgMAH was used finer PP particles seem to disperse in the PA6 domain as compared to blends with PPgMAH (average of PP particles diameter of 1.20 μm for POEgMAH and 2.34 μm for PPgMAH). Tucker et al. [6] reported similar observation in the cases of 20% PA6 and 1% SEBSgMAH: The SEBSgMAH provides better wetting with PA6 than PPgMAH did, which leads to an improvement in adhesion to the PP matrix. According to Rosch and Mulhaupt [11] on compatibilized PP/PA blends by SEBSgMAH or EPMgMAH, the maleated elastomer acted as a dispersing agent that reduced the average diameter of dispersed PA in PP matrix. The reduction in PA dispersed size was attributed by formation of core shell PA/SEBSgMAH where maleated rubber was located at the interfaces. Smaller particle sizes of dispersed PA appears to be efficient stress concentrators resulting in higher impact strength. Furthermore, it is believed that the viscosity difference between POEgMAH and PPgMAH is another factor for the morphological difference. As suggested by Chow et al. [13] the melt viscosity of EPRgMAH rubber is higher than PPgMAH and this would affect the viscosity difference between nanocomposites with rubber and PPgMAH, producing a different morphology.

Thermal Analysis

Differential Scanning Calorimetry (DSC)

Figure 9 shows the DSC heating scans of uncompatibilized and compatibilized PA6/PP nanocomposites. The values of melting temperature

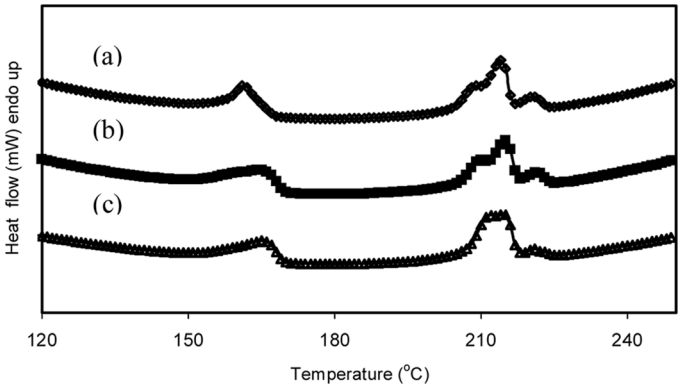

FIGURE 9 Melting endotherms of PA6/PP blends (a) uncompatibilized nanocomposites and compatibilized (b) PPgMAH, (c) POEgMAH.

(T_m), crystallization temperature (T_c) and crystallinity content are given in Table 3. It is seen from Figure 9 that the PA6 in PA6/PP nanocomposites had two melting peaks, the high temperature corresponds to the melting point of crystalline α form and the low temperature peak corresponds to melting point of the γ form [20–21]. No significant changes of melting peak were observed for PA6 after the incorporation of compatibilizer in the composites, regardless of whether it is PPgMAH or POEgMAH. On the other hand, T_m of PP increased with the presence of compatibilizer, which indicates an interaction between compatibilizer, which is olefin based, and PP. An increase in T_m of PP suggests that PP formed a large and more regular lamellae resulted in a more perfect crystal that led to the higher melting temperature. This is consistent with the results obtained by Li et al. [22]. They reported that increase in T_m of PP was observed in PP-EPR blends and PP-ULDPE blends. They interpreted such observation as a partial dissolution of the defective molecules of PP in the EPR and ULDPE. PP might form large and more

TABLE 3 Values of T_m, T_c, and X_c for PA6/PP Blends, Uncompatibilized and Compatibilized Nanocomposites

	T_m (°C)		T_c (°C)		Crystallinity, X_c (%)	
	PA	PP	PA	PP	PA	PP
PA6/PP/FA4	214.1	161.5	187.0	117	33.0	34.5
PA6/PP/FA4/C5	214.9	165.1	188.6	102	30.3	33.6
PA6/PP/FA4/E10	214.6	165.4	190.7	95,105	28.8	33.2

regular lamellae because of a narrower molecular weight distribution and fewer defective molecules. As a result, a prefect crystal was formed that led to the higher melting temperature.

The crystallization exotherms observed during cooling from the molten state of uncompatibilized and compatibilized PA6/PP nanocomposites are shown in Figure 10. It can be seen that the addition PPgMAH in the blends decreased the T_c of PP, which indicates slowing of PP crystallization. A similar observation was reported by Lee and Yang [8] and Campoy 1995 et al. [23] on PP/PA6 compatibilized by various content of PPgMAH. The decrease was attributed to the hindrance arising from the formation of graft copolymer.

For POEgMAH compatibilized nanocomposites, two peaks were observed at 95°C and 105°C. Lee and Yang [8] reported similar results with the addition of 2.5% PPgMAH in PA dominant PA/PP blends. The decrease in T_c of PP was attributed to the co-crystallization of copolymer formed during the melt blending. The co-crystallization is indicative of the good interfacial adhesion between PA6 and PP in the presence of POEgMAH. Similar results would be expected for PPgMAH. However, POEgMAH have better adhesion with PP due to chemical similarity between POEgMAH and the PP used in this study, as compared to PPgMAH. The presence of ethylene phase in PP heterophasic copolymer used in this study may further improve the compatibility between POE and PP matrix [24]. No significant changes in T_c was observed for PA with the addition of PPgMAH. However, higher T_c was obtained for POEgMAH compatibilized

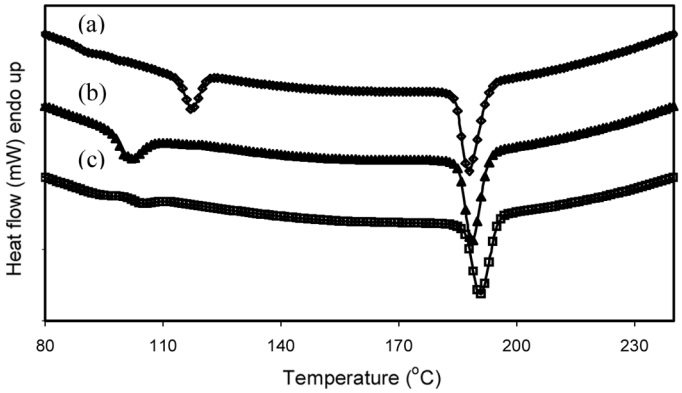

FIGURE 10 Crystallization exotherms of PA6/PP blends (a) uncompatibilized nanocomposites and compatibilized (b) PPgMAH, (c) POEgMAH.

blends. This may be due to the altered nucleation and crystal growth in presence of PA6gPOE copolymer.

As can be seen in Table 3, the incorporation of compatibilizer (POEgMAH or PPgMAH) decreased the crystallinity of PA6 in PA6/PP nanocomposites. This is believed to be due to a better interfacial adhesion in the compatibilized blends. The copolymers formed located at the interface may able to suppress the crystal formation.

CONCLUSIONS

The compatibilizing effects on the mechanical properties and morphology of PA6/PP nanocomposites have been investigated. PPgMAH and POEgMAH used in blends improved the compatibility between PA6 and PP. The impact strength of POEgMAH compatibilized nanocomposites are up to two times higher than PPgMAH compatibilized PA6PP nanocomposites. However, the PPgMAH compatibilized PA6PP nanocomposites have higher tensile strength and Young's modulus compared to nanocomposites compatibilized by POEgMAH. Both compatibilizers significantly reduced the water absorption. Molau test and FTIR proved the formation of copolymer linkage in the compatibilized blends. XRD analysis showed that organoclay was already exfoliated in the uncompatibilized PA6/PP nanocomposite. No significant change was observed upon addition of the compatibilizer. The SEM confirmed that PP was uniformly distributed in PA6 matrix with the incorporation of PPgMAH or POEgMAH. Through DSC study, it was found that the melting and cooling behavior of the PA6/PP nanocomposites were modified by the addition of compatibilizer.

REFERENCES

[1] Ray, S. S. and Okamoto, M., *Progress in Polymer Science* **28**, 1539 (2003).
[2] Wu, Z., Zhou, C., and Zhu, N., *Polymer Testing* **21**, 479 (2002).
[3] Cho, J. W. and Paul, D. R., *Polymer* **42**, 1083 (2001).
[4] Ohlsson, B., Hassander, H., and Tornell, B., *Polymer* **39**, 6705 (1998).
[5] Roeder, J., Oliveira, R. V. B., Goncalves, M. C., Soldi, V., and Pires, A. T. N., *Polymer Testing* **21**, 815 (2002).
[6] Tucker, J. D., Lee, S., and Einsporn, R. L., *Polymer Engineering and Science* **40**, 2577 (2000).
[7] Chow, W. S., Ishak, Z. A., Kocsis, J. K., Apostolov, A. A., and Ishiaku, U. S., *Polymer* **44**, 7427 (2003).
[8] Lee, J. D. and Yang, S. M., *Polymer Engineering and Science* **35**, 1821 (1995).
[9] Zeng, N., Bai, S. L., Sell, C. G., Hiver, J. M., and Mai, Y. W., *Polymer International* **51**, 1439 (2002).
[10] Chow, W. S., Ishak, Z. A., Kocsis, J. K., Apostolov, A. A., and Ishiaku, U. S., *European Polymer Journal* **41**, 687 (2005).

[11] Rosc, J. and Mulhaupt, R., *Polymer Bulletin* **32**, 697 (1994).
[12] Bai, S. L., Wang, G. T., Hiver, J. M., and G'Sell, C., *Polymer* **45**, 3063 (2004).
[13] Chow, W. S., Ishak, Z. A., Kocsis, J. K., Apostolov, A. A., and Ishiaku, U. S., *Macromolecules Materials Engineering* **209**, 122 (2005).
[14] Hassan, A., Othman, N., Wahit, M. U., Wei, L. J., Rahmat, A. R., and Ishak, Z. A., *Macromolecular Symposia* **239**, 182 (2006).
[15] Li, Z., Guo, S. Y., Song, W. T., and Hou, B., *Journal of Materials Science* **38**, 1793 (2003).
[16] Tseng, F. P., Lin, J. J., Tseng, C. R., and Chang, F. C., *Polymer* **42**, 713 (2001).
[17] Huang, Y., Liu, Y., and Zhao, C., *Journal of Applied Polymer Science* **69**, 1505 (1998).
[18] Yu, Z. Z., Ou, Y. C., and Hu, G. H., *Journal of Applied Polymer Science* **69**, 1711 (1998).
[19] Li, F., Chen, Y., Zhu, W., Zhang, X., and Xu, M., *Polymer* **39**, 6929 (1998).
[20] Devaux, E., Bourbigot, S., and Achari, A.E., *Journal of Applied Polymer Science* **86** 2416 (2002).
[21] Fornes, T. D. and Paul, D. R., *Polymer* **44**, 3945 (2003).
[22] Li, J., Shanks, R. A., and Long, Y., *Journal of Applied Polymer Science* **87**, 1179 (2003).
[23] Campoy, I., Arribas, J. M., Zaporta, M. A. M., Marco, C., Gomez, M. A., and Fatou, J. G., *European Polymer Journal* **31**, 475 (1995).
[24] Paul, S. and Kale, D. D., *Journal of Applied Polymer Science* **76**, 1480 (2000).